Diamond & Related Materials 23 (2012) 50–53

Contents lists available at SciVerse ScienceDirect

Diamond & Related Materials

journal homepage: www.elsevier.com/locate/diamond

Computer simulations of nanostructured carbon under tensile load: Electronic structure and optical gap

Christos Mathioudakis [a], Maria Fyta [b,*]

[a] Department of Materials Science and Technology, University of Crete, P.O. Box 2208, 71003 Heraklion, Crete, Greece
[b] Physics Department (T37), Technical University of Munich, 85748 Garching, Germany

ARTICLE INFO

Available online xxxx

Keywords:
Amorphous carbon
Composites
Diamond crystal
Nanocrystalline
Simulation
Optoelectronic properties
Strain
Coatings
Optical properties

ABSTRACT

We use computer simulations to study the behavior of amorphous carbon and carbon composites under tensile strain. We investigate the behavior of the optoelectronic properties of these materials as strain is increased. These properties are monitored through the electronic density of states, the optical gap and the Urbach energy for both materials. The variation in the hybrid (sp^2 and sp^3) content due to the external load is directly connected to changes in the optoelectronic properties with increasing strain. This connection will lead to interesting features in the Urbach edge for the amorphous network, while the respective effect for the nanocomposite will be less pronounced. The situation is reversed when the optical gap is used as a probe of the properties of both amorphous and composite materials.

1. Introduction

The quest for materials with tunable properties has been desirable in view of the respective large impact on the related nanotechnological applications. Within the carbon family of structures, amorphous and nanocomposite carbon show a promise in generating materials with tunable mechanical and optoelectronic properties. Specifically, tetrahedral carbon (t*a*-C), a dense amorphous network which contains a high fraction of sp^3 hybrids [1,2] shows high rigidity and diamond-like optoelectronic properties [1,3,4], which can be varied according to the sp^3 content. Similar is the case for nanocomposite diamond, which includes a crystalline diamond core surrounded by an amorphous carbon matrix and has recently attracted attention [5]. Such structures, have already been grown in both hydrogenated [6] and hydrogen-free [7] amorphous carbon, and have been also theoretically investigated [8,9]. The choice of the size of the embedded diamond and the amorphous matrix density can lead to a composite material with desired properties. Note, that with the term "diamond" we refer to the perfect, tetrahedral diamond crystal. Hybrids of an sp^3 nature can also form clusters in an amorphous network. In such a case, the properties, such as the rigidity are not solely dependent on the sp3 content, but depend on the clustered hybrids as well [10]. The appropriate choices in both amorphous and composite materials can also generate materials with diamond-like properties. In this respect, dense amorphous and nanocomposite networks have interesting nanotechnological applications as hard and wear resistance coatings [11,12] with hardness and thermal stability comparable to that of diamond. Nanostructured carbon materials show also a promise for applications in microelectromechanical devices.

In view of these applications, in this work, we aim to investigate how specific properties of two carbon forms, tetrahedral amorphous carbon (t*a*-C) and dense diamond nanocomposites (*n*D/*a*-C) are affected by the application of strain up to their fracture points. As a probe, we will briefly discuss their electronic density of states (e-DOS), the variation of the Urbach energy (E_U), and the optical gaps as a function of the decreasing four-fold (sp^3) content in these networks. E_U also serves as a measure of disorder in the structures. We will show that the e-DOS will essentially show no interesting features as strain is increased, as opposed to the case of E_U and the optical gap. This paper will be structured as follows: In Section 2 we briefly discuss the methodology that has been used for the current investigation, we then move on to the discussion of the results in Section 3 and conclude in Section 4.

2. Methodology

For the present investigation, the NRL tight-binding molecular dynamics (TBMD) has been used [13]. It involves a non-orthogonal tight-binding model and uses distance- and environment-

* Corresponding author.
E-mail addresses: chrm@materials.uoc.gr (C. Mathioudakis), mfyta@ph.tum.de (M. Fyta).

0925-9635/$ – see front matter © 2011 Published by Elsevier B.V.
doi:10.1016/j.diamond.2011.12.044

dependent parameters for transferability. This methodology has been previously proven efficient in relevant studies of amorphous and nanostructured carbon, also off-equilibrium [8]. This scheme is more accurate than classical methods, but also provides a higher statistical accuracy than first-principles schemes. It also describes well quantum-mechanical effects, such as bond-breaking discussed in this work. Additional details to the NRL scheme can be found elsewhere [14].

2.1. Structure generation and calculation of optoelectronic properties

Computational supercells with periodic boundary conditions of 216 and 512 atoms are used to model t*a*-C and the diamond nanocomposite, respectively. All networks have been generated through the liquid-quench method, i.e. by melting an initial diamond crystal and subsequently quenching the melt at constant volume in a canonical (N,V,T) ensemble. In the case of the diamond nanocomposites, during the melting and quenching phases the atoms that belong to the diamond inclusion are kept frozen. After quenching, the respective part of the material has become amorphous and both atomic positions and volumes are equilibrated at low temperatures. The density and hybridization content in both materials are controlled by the volume of the computational cell during quenching. This allowed the formation of sp^2 hybrids without the involvement of any graphitic-like structure. Additional details on the network generation can be found elsewhere [8,15,16]. Here, we focus on two dense networks, a diamond nanocomposite with a diamond inclusion of about 1.25 nm in diameter, with a volume fraction of 31% and a matrix density of 3 g cm^{-3} which corresponds to a mean coordination of 3.8 in the amorphous matrix. We apply tensile strain along the ⟨111⟩ direction, which coincides with the easy-slip plane of diamond. The structures are strained in incremental strain. At the end of each straining step, all atomic positions are allowed to relax and the properties are extracted at 0 K. In principle, since the amorphous networks are highly isotropic, different straining directions for these networks are equivalent [8]. Both networks fracture at a strain of about 0.11–0.12 [8].

As already mentioned, we are interested in the changes in the optoelectronic properties of the strained t*a*-C and the diamond nanocomposite. For the analysis of these properties, we follow the methodology adapted for similar unstrained networks from [9]. Briefly, the approach was based on extracting the electronic structure from the simulations. This is then directly correlated to the imaginary part of the dielectric function of the material, which is given as a sum over all matrix elements corresponding to transitions from an initial occupied to a final unoccupied state. Knowledge of the imaginary part of the dielectric function directly leads to the absorption coefficient (α) and the optical gap (E_{04}). The absorption coefficient in turn is used to compute to the Urbach energy (E_U), which is a link of the disorder in the structures. This method has been proven efficient and has also passed the consistency checks for diamond. Detailed information on this procedure can be found elsewhere [9].

3. Results and discussion

We follow the methodology described in the previous section and look at specific properties of the strained amorphous and diamond nanocomposite networks. We first investigate the hybridization content in these structures, move on to the electronic density of states and the variation of the optical gap and Urbach energy with the four-fold ratio.

3.1. Hybridization content and e-DOS

It is physically intuitive that as strain is applied, the bonds are elongated and eventually break. In a dense four-folded network this is interpreted as rendering many of the sp^3 hybrids into sp^2 ones. We have observed, that a small amount of sp^3 hybrids do break into sp^2 ones. The criterion for assigning a bond as broken is that its length should be longer that the distance corresponding to the first minimum of the pair distribution function. This reflects the fact that the majority of the sp^3 bonds in the strained networks are elongated rather than broken. It is interesting to observe that the mechanical behavior under tensile load for both networks is quite similar, in the sense that the majority of bonds that break are the sp^3 ones of the t*a*-C network and the sp^3 hybrids of the amorphous matrix in the nanocomposite. The results for both networks are summarized in Fig. 1. It is evident, that there is only a small change in the sp^2 and sp^3 contents in the strained structures, though these eventually fracture, as mentioned above. The sp^3 ratio in the strained t*a*-C decreases slightly more than in the strained diamond nanocomposite. This small difference is based on the fact that the nanocomposite consists also of a highly ordered phase – the diamond inclusion – which cannot be easily deformed. Such a highly ordered region does not exist in t*a*-C, even if some clustered close to tetrahedral symmetry sp^3 atoms can be found also in t*a*-C. We have indeed seen, that under tensile load the diamond core of the nanocomposite is kept almost intact, while bonds in the matrix break and deform. Only the interface atoms are slightly affected by the application of strain, at least up to the fracture point of the whole material.

We begin the derivation of the optoelectronic properties by evaluating the electronic structure of the strained networks. Looking at the total electronic density of states (e-DOS) as a function of the applied strain ε for both networks does reveal specific features as ε is increased. It is expected that decomposition of the total e-DOS into contributions from the different hybrids will reveal a small increase in the π, $\pi^\star$ states within the gap. The increasing distorted sp^3 bonds will also become more evident in the gap region. Fig. 2 represents the total e-DOS for both the diamond nanocomposite and t*a*-C without strain and when these fracture. For the composite, at $\varepsilon=0$, the band separation is still distinct and filled mainly by defect states coming from the distorted bonds at the inclusion-matrix interface. The $\sigma-\sigma^\star$ gap is controlled by the amorphous matrix part having in principle a lower gap than diamond due to the sp^2 atoms. For a large strain ($\varepsilon=0.12$ in panel (b)), π, $\pi^\star$ states coming from the increased sp^2 atoms in the matrix start slightly to be visible. An additional increase of the distorted bonds at the interface leads to the shrinking of the gap. In t*a*-C (panels (c) and (d)), in the strained case ($\varepsilon=0.12$) the three-fold states around the $\sigma-\sigma^\star$ gap become more evident than for $\varepsilon=0$. The $\pi^\star$ peaks, which also occur for $\varepsilon=0$ are more pronounced at higher strains. This behavior, i.e. the shrinking of the band-gap would become more evident as the strain is increased above the fracture point of both amorphous and

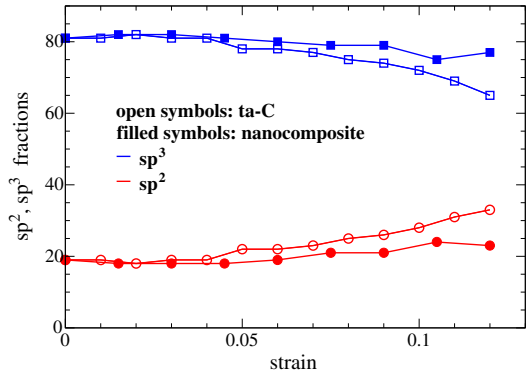

Fig. 1. Hybrid content with applied strain for both the nanocomposite (filled symbols) and amorphous (open symbols) networks. Squares and circles show the sp^3 and sp^2 ratio, respectively.

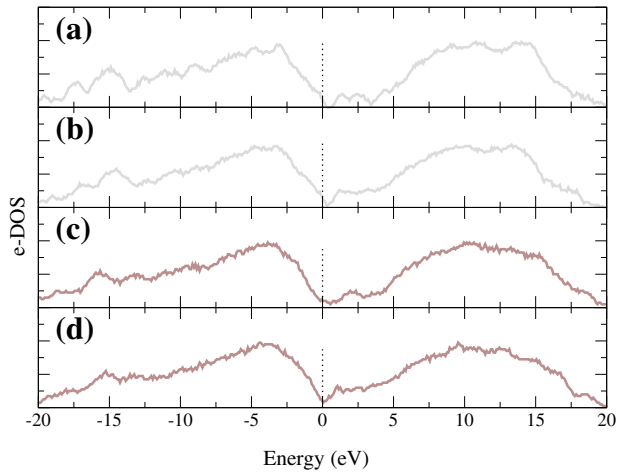

Fig. 2. Total e-DOS for the diamond nanocomposite and the t*a*-C network. In (a), (b) results are shown for the diamond composites at 0 and 0.12 strain, respectively. In (c), (d) the respective results for the same amount of load are shown for t*a*-C. The e-DOS is shifted, so that 0 eV corresponds to the Fermi energy (black/dotted line).

composite materials. From a nanotechnological point of view, though, going beyond the fracture point would not be of high interest.

3.2. Optical gap and Urbach energy

We move on to the variation of the optical gap and the Urbach energy with the total sp^3 content in the structures. The results for the diamond nanocomposite are depicted in Fig. 3. Note, that the same sp^3 content may correspond to different strains, hence the multiple values of the gap or E_U for the same sp^3 ratio. For the strained diamond nanocomposite, the optical gap vs. sp^3 ratio curve is about 0.5 eV lower than the respective unstrained case [9]. Evidently, the deformations due to strain, specifically at the interface region, lead to significant deviations from tetrahedral symmetry as compared to unstrained composites. These deviations, as shown through the optoelectronic properties in the simulated structures, would be of practical interest in applications as these could be directly observable in the experiments the way it is proposed in this work. The overall decrease in the optical gap shown in the figure is about 0.55 eV, larger than in strained t*a*-C, which will be discussed next. The values for the Urbach energy of the strained composite are slightly lower than in the unstrained diamond composites [9]. This might occur due to the interplay of regions of different density and hybridization content in the strained structures. The variation lies also in the same range as the Urbach energy for core atoms in the unstrained diamond composites for the same range of sp^3 content [9].

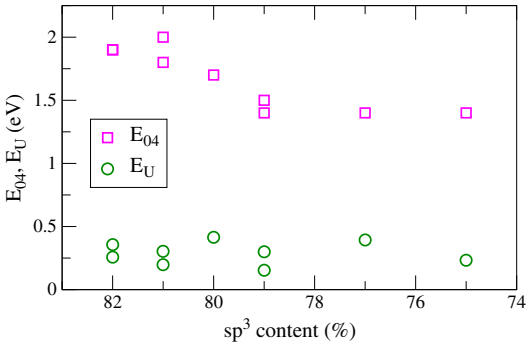

Fig. 3. Variation of the optical gap E_{04} (squares) and the Urbach edge E_U (circles) with the sp^3 content in the diamond nanocomposite.

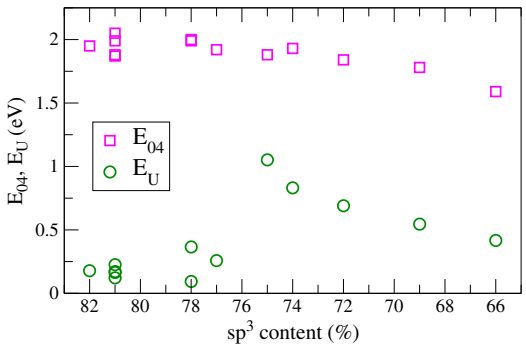

Fig. 4. Variation of the optical gap E_{04} (squares) and the Urbach edge E_U (circles) with the sp^3 content in t*a*-C.

In the case of t*a*-C, the results of which are shown in Fig. 4, the optical gaps are quantitatively similar to those for the unstrained case for the same four-fold content (see [4]). The optical gap decreases as the four-fold content decreases. The overall decrease is about 0.35 eV, which is not very large taking into account that the sp^3 bonds are unphysically elongated and distorted in the strained material. The Urbach edge as a function of the four-fold content in the strained amorphous network follows the non-monotonic behavior of the unstrained non-hydrogenated amorphous networks [4]. It also increases sharply, reaching a maximum and then declines sharply. This feature reveals a mechanism affecting the Urbach energy of strained dense amorphous carbon, which is similar to that for unstrained amorphous networks with a varying sp^3 content.

4. Conclusions

In this work we have applied tensile strain on dense amorphous and diamond nanocomposite networks using a tight-binding molecular dynamics computational scheme. We have investigated how the external load affects different properties of these materials. As a result, we found no significant change in their electronic density of states, since the change in the hybridization content was not significant. The decrease of the four-fold content in these structures, though, led to a noticeable difference in their optical gap and Urbach edge as compared to the equilibrium unstrained structures. We have investigated the connection of both the Urbach energy and the optical gap with the sp^3 content in the strained materials. In the amorphous case, larger deviations from the unstrained network were found in the Urbach energy, while no significant change was evident in the optical gap. On the other hand, for the diamond nanocomposite, a larger decrease in the optical gap was clear compared to a very small variation in the Urbach energy. Conclusively, such properties can serve as a probe for possible deformations or fracture in such nanostructured networks. Here, the aim was to set a pathway to recognize these structural alterations affecting the operation of functional materials in practical nanotechnological applications.

Acknowledgements

MF acknowledges support from the 'Gender Issue Incentive Funds' of the Cluster of Excellence in Munich, Germany and the 'BioFuS' project of the Intra-European Marie-Curie Actions (call FP7-PEOPLE-2009-IEF).

References

[1] J. Robertson, Mater. Sci. Eng. R (2002) 129.
[2] S.R.P. Silva, in: H.S. Nalwa (Ed.), Handbook of Thin Film Materials, Vol.4, Academic Press, New York, 2002, p. 403.
[3] P.C. Kelires, Phys. Rev. Lett. (1994) 2460.

[4] C. Mathioudakis, G. Kopidakis, P. Patsalas, P.C. Kelires, Diam. Relat. Mater. (2007) 1788.
[5] Y. Lifshitz, T. Kohler, T. Frauenheim, I. Guzmann, A. Hoffman, R.Q. Zhang, X.T. Zhou, S.T. Lee, Science (2002) 1531.
[6] Y. Lifshitz, et al., Science (2002) 1531.
[7] Y. Yao, M.Y. Liao, T. Kohler, T. Frauenheim, R.Q. Zhang, Z.G. Wang, Y. Lifshitz, S.T. Lee, Phys. Rev. B 72 (2005) 035402.
[8] M. Fyta, P.C. Kelires, Phys. Rev. Lett. 96 (2006) 185503.
[9] G. Vantarakis, C. Mathioudakis, et al., Phys. Rev. B 80 (2009) 045307.
[10] H.-S. Zhang, J.L. Endrino, A. Anders, Appl. Surf. Sci. 255 (2008) 2551.
[11] A.A. Voevodin, J.S. Zabinski, Diamond Relat. Mater. (1998) 463.
[12] D. Neerinck, P. Persoone, M. Sercu, A. Goel, C. Venkatraman, D. Kester, C. Halter, P. Swab, D. Bray, Thin Solid Films 317 (1998) 402.
[13] R.E. Cohen, M.J. Mehl, D.A. Papaconstantopoulos, Phys. Rev. B (1994) 14694.
[14] D.A. Papaconstantopoulos, M.J. Mehl, J. Phys. Condens. Matter (2003) R413.
[15] C. Mathioudakis, G. Kopidakis, P.C. Kelires, C.Z. Wang, K.M. Ho, Phys. Rev. B (2004) 125202.
[16] M.G. Fyta, I.N. Remediakis, P.C. Kelires, Phys. Rev. B (2003) 035423.